An *ab Initio* Quantum Mechanical Model for the Catalytic Mechanism of HIV-1 Protease

Hsing Lee,*,† Thomas A. Darden,† and Lee G. Pedersen‡

Contribution from the Laboratory of Quantitative and Computational Biology, National Institute of Environmental Health Science, Research Triangle Park, North Carolina 27709, and Department of Chemistry, University of North Carolina, Chapel Hill, North Carolina 27599-3290

Received April 25, 1995. Revised Manuscript Received January 19, 1996[⊗]

Abstract: The catalytic mechanism of the HIV-1 protease (HIV-PR) is studied through *ab initio* theoretical model calculations. This model consists of a formate/formic acid pair, a structurally important water molecule, and a formamide molecule. The proposed catalytic mechanism is composed of five steps, two of which are transition states separated by a third step (an intermediate state). The remaining two steps are related to product release. The overall forward hydrolysis reaction barrier is approximately 22 kcal/mol, with a reverse hydrolysis barrier of approximately 34 kcal/mol at the RHF/6-31G* level. The second transition state is related to a nucleophilic attack of the water molecule on the carbon atom of the substrate scissile bond, and is essential for the collapse of the substrate. That the transition state structures of HIV-PR have not been identified makes a theoretical study of this kind particularly valuable for understanding the HIV-PR mechanism.

Introduction

HIV type 1 protease (HIV-PR) is a 99-amino acid protein that is crucial for the maturation of the HIV virion. HIV-PR catalyzes its own release from the poly-protein $Pr160^{gag\text{-}pol}$, the protein product of HIV-DNA, by hydrolysis of certain peptide bonds. Once free, the PR catalyzes a series of hydrolytic cleavages resulting in the final proteins of the matured form of the HIV virus.[1] It has been found[2] that effective inhibition of HIV-PR leads to production of a noninfectious form of the virus. These considerations make HIV-PR an attractive therapeutic target.

The active site triad Asp-Thr-Gly (residues 25−27) of HIV-PR is characteristic of aspartic proteases, a well-known family of proteases. The active form of HIV-PR is dimeric, the structural details of which became clear after the determination of the crystal structure of a synthetic HIV-PR at a resolution of 2.8 Å by Wlodawer *et al.*[3] It follows from this structure that the two side chains of Asp-25 and Asp-25′ of the active site are planar with a structural water molecule bound to both. Meek and co-workers[4] presented evidence from kinetic studies that at physiological conditions one of the carboxylate groups of the aspartate side chains is protonated while the other is not. The water molecule has been postulated to carry out the nucleophilic attack on the C atom of the substrate scissile bond. The role for the rest of the active site triad remains unclear. In the X-ray crystallographic structure of HIV-PR, the N atoms of Gly-27 and Gly-27′ are in a position to form H-bonds to the O_δ atoms of D25/D25′. However, experiments to date appear to indicate that these glycine residues do not participate in the catalysis directly. It may be reasonable to assume that glycine 27 and glycine 27′ are responsible for maintaining the planarity of the D25/D25′ motif.

It appears from the isotope kinetic experiments[4] that two major components are involved in the HIV-1 PR catalysis. First, proton transfers involving both the scissile nitrogen and carbon atoms of the substrate are involved during the hydrolysis. Second, an additional water molecule participates in the product release. While these factors are inconsistent with some earlier mechanisms that have been proposed,[8] two proposals appear to be the most plausible. The essence of the proposal by Meek and co-workers,[4b] which we have not evaluated in this study, is the formation of an amide hydrate intermediate involving the lytic water molecule and several concerted proton transfers. This proposal will ultimately be interesting to study with theoretical calculations.

The current theoretical study has been formulated to follow closely the proposal by Jaskolski *et al.*[9] The original assumptions of this proposal are the following: (1) A concerted electrophilic attack of a proton of the active site on the target nitrogen atom of the substrate scissile bond together with a nucleophilic attack of the water molecule on the C atom of the substrate peptide bond start the reaction and lead to a transition state. (2) The cleaved acetyl-terminal product binds to the two inner oxygen atoms ($O_{\delta 1}$ and $O_{\delta 1'}$ in Figure 1) of the aspartates

* To whom correspondence should be addressed.
† National Institute of Environmental Health Science.
‡ University of North Carolina.
⊗ Abstract published in *Advance ACS Abstracts,* March 15, 1996.

(1) Henderson, L. E. *et al.* in *Human Retroviruses, Cancer and AIDS: Approach to Prevention and Therapy*; Alan R Liss, Inc.: New York, 1988; pp 135−147. Debouck, C. *et al. Proc. Natl. Acad. Sci. U.S.A.* **1987**, *84*, 8903−8906.
(2) Kohl, N. E. *et al. Proc. Natl. Acad. Sci. U.S.A.* **1988**, *85*, 4686−4690.
(3) Wlodawer, A. *et al. Science* **1991**, *245*, 616−621.
(4) (a) Hyland, L. J.; Tomaszek, T. A.; Meek, T. D. *Biochemistry* **1991**, *30*, 8454−8463, 8441−8453. (b) Rodriguez, E. J.; Angeles, T. S.; Meek, T. D. *Biochemistry* **1993**, *32*, 12380−12385.
(5) Shaik, S. S.; Schlegel, H. B.; Wolfe, S. *Theoretical Aspects of Physical Organic Chemistry*; Wiley: New York, 1992. Eksterowicz, E. J.; Houk, K. N. *Chem. Rev.* **1993**, *93*, 2439−2461.
(6) Scherner, S. *et al. Int. J. Quantum Chem.* **1983**, *23*, 739.
(7) Frisch, M. J. *et al.* Gaussian 92/DFT, Rev. F3; Gaussian Inc.: Pittsburgh, PA, 1993.
(8) Kay, J. In *Aspartic Proteinases and Their Inhibitors*; Kostka, V., Ed.; de Gruyter: Berlin, 1985; pp 1−17. James, M. N. G.; Sielecki, A. R. *Biochemistry* **1985**, *24*, 3701−3713. Polgár, L. *FEBS Lett.* **1983**, *219*, 1−4. Pearl, L. H. *FEBS Lett.* **1987**, *214*, 8−12. Abeles, R. H.; Frey, P. A.; Jencks, W. P. *Biochemistry*; Jones and Bartlett Publishers: Boston, 1992; p 161. Suguna, K.; Padlan, E. A.; Smith, C. W.; Carlson, W. D.; Davies, D. R. *Proc. Natl. Acad. Sci. U.S.A.* **1987**, *87*, 7009−7013. James, M. N. *et al. Biochemistry* **1987**, *31*, 3872−3886.
(9) Jaskolski, M.; Tomasselli, A. G.; Sawyer, T. K.; Staples, D. G.; Heinrikson, R. L.; Schnerider, J.; Kent, S. B.; Wlodawer, A. *Biochemistry* **1991**, *30*, 1600−1609.

0002-7863/96/1518-3946$12.00/0

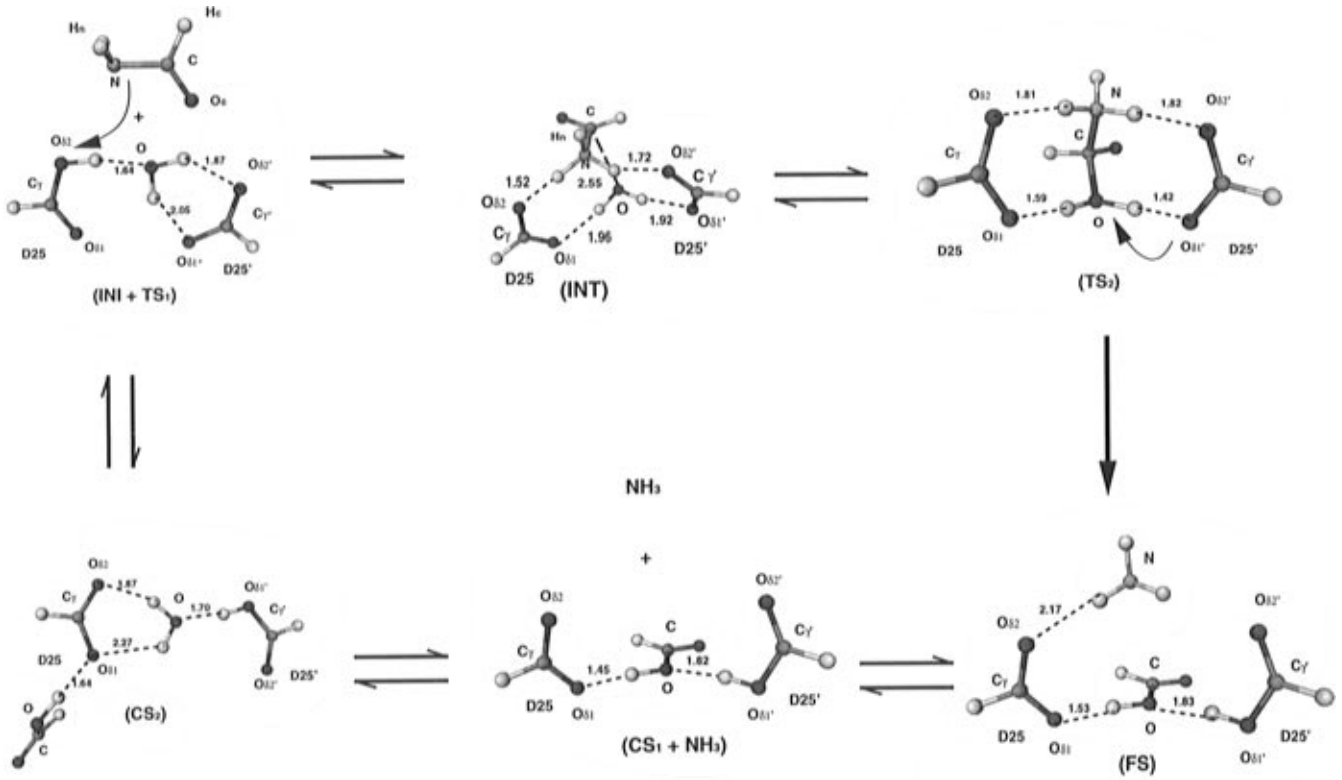

Figure 1. Structural description of the proposed catalytic reaction path of the HIV-PR. The descriptions of the structures are given in sequence according to the order described in the text. See text for the definition of each step. Dotted lines indicate potential hydrogen bonds, arrows indicate proton transfer. The structures are from the RHF/6-31G* optimizations.

of the PR after the hydrolysis, a detail that has been neglected in most proposals. The first assumption of Jaskolski *et al.* differs from several others[8] in that the target of the electrophilic attack is the nitrogen atom of the substrate peptide bond rather than the peptide oxygen of the substrate. The key step in the mechanism is the transition state that is related to the nucleophilic attack of the structural water molecule on the C carbon atom of the substrate peptide bond.[9]

Methods

In principle, quantum mechanics can provide an atomic level understanding of how chemical reactions proceed. The keys to such an understanding are the locations of the energy barriers that define the transition states.[5] Of essential interest here is the complete proteolytic cycle in which the substrate peptide bond is broken during the normal hydrolysis involving HIV-PR. Two factors limit quantum chemistry studies of this kind: the size of the molecular system and the accuracy of the different levels of theory. In the case of HIV-PR, a proper description of the H-bonds appears to be essential, and so a relatively high level of theory is required. That the RHF/4-31G[6] or higher level of theory is desirable forces our molecular model to be a small one: a formic acid/formate anion pair (denoted as D25/D25′ here) with a structurally important water molecule bound to represent the active site motif. The substrate model is chosen to be a formamide molecule.

All *ab initio* calculations employed in this study use the GAUSSIAN 92/DFT[7] suite of programs. The structures were optimized with analytical energy derivatives with both basis sets RHF/4-31G and RHF/6-31G*. The reasonableness of the RHF/6-31G* basis set is supported by the fact that the $\Delta H°_{rxn}$(298 K) for formamide (g) + H_2O → ammonia (g) + formic acid (g) is 2.5 kcal/mol for the 6-31G* basis set, whereas the experimental value is 3.4 kcal/mol. The MP2 energies are single-point calculations for the respective RHF/6-31G* optimized structures for the larger complexes, and with analytical force optimizations for most small molecules. The full core hamiltonian was used for all MP2 calculations. The higher level optimizations took the optimized structures from the previous level as the starting ones.

Description of the Reaction Pathway

Several quantum chemistry studies[10,11] of the aspartic proteases have focused mostly on the stable conformations (energy minima) of the active site of the proteases, with different possible protonation states. We started the optimization of the HIV-PR structure from the crystallographic information. The conformation we adapted below for the protease active site is the energy minimum among all the possibilities studied.[11]

1. Initial State (INI and TS_1). The geometries of the two separated structures for the model substrate and the modeled active site of HIV-PR were optimized with respect to energy at the beginning.

(a) Substrate. The modeled substrate is a formamide molecule. We optimized first at the RHF/4-31G level, then at the RHF/6-31G*, and subsequently reoptimized at the MP2/6-31G* level. The ground state of this molecule is planar. This molecule, however, has a transition state form that is important in describing the reaction path. The transition state structure (TS_1) of this molecule is approximately tetrahedral at the nitrogen atom so that the electron lone pair takes one of the sp^3 orbitals. This transition state has a remarkable charge redistribution so that the scissile peptide bond strength is significantly

(10) Goldblum, A. *J. Comput. Chem.* **1987**, *8*, 835. Goldblum, A. *Biochemistry* **1988**, *27*, 1653. Hadzi, D. *J. Mol. Struct.* **1987**, *150*, 241−250; **1988**, *181*, 71−80. Goldblum, A. *et al. Theor. Chim. Acta* **1993**, *85*, 231−247. Ciarkowski, J.; Oldziej, S.; Liwo, A. *Polish J. Chem.* **1994**, *68*, 939−947, 949−956. Aleksandrov, S. L.; Antonov, K. *Soviet J. Bioinorg. Chem.* **1990**, *16*, 245−254.

(11) Beveridge, A. J.; Heywood, G. C. *Biochemistry* **1993**, *32*, 3325−3333. Beveridge, A. J.; Heywood, G. C. *J. Mol. Struct.* **1994**, *306*, 235−247.

(12) Wiberg, K. B.; Laidig, K. E. *J. Am. Chem. Soc.* **1987**, *109*, 5935−5943. Wiberg, K. B.; Breneman, C. M. *J. Am. Chem. Soc.* **1992**, *114*, 831−840. Bach, R. D.; Mintcheva, I.; Kronenberg, W. J.; Schlegel, H. B. *J. Org. Chem.* **1993**, *58*, 6135−6138.

reduced ($\Delta R_{C-N} = 0.08$ Å at RHF/6-31G*, changing from partly a double-bond to a more or less single bond), and is therefore crucial in modeling the hydrolysis process (see below). Wiberg has shown[12] that this change is related to the internal rotational energy barrier of the molecule.

(b) Active Site Model. The active site model complex consists of a formate/formic acid pair and a structurally important water molecule. The model was built from the heavy atoms of the active site of the X-ray structure of HIV-PR. From each monomer of the HIV-PR molecule, we deleted all atoms except the side chain atoms of D25 and then changed the C_β carbons to hydrogen atoms to reduce the model size. A proton was added to one of the two D25 side chains, to comply with the experimental protonation states. The structural water was built from its crystallographic oxygen position, which is also consistent with Jaskolski *et al.*'s model.[9] The starting active site model was constrained to be co-planar with a $C_\gamma - C_{\gamma'}$ distance of 5.28 Å. After the initial optimization, the $C_\gamma - C_{\gamma'}$ distance constraint was relaxed. The optimized structures are given in Figure 1 (INI). The resulting optimized geometry is similar to that reported in earlier quantum chemical calculations.[10,11]

2. Intermediate State (INT). The optimized model substrate and model active site were brought together (Figure 1) so that the N (substrate)$-O_{\delta 2}$ (active site) distance was approximately 3.1 Å, and the C carbon (substrate)$-$O (water) distance was approximately 3.2 Å. To avoid a spurious hydrogen bond, two constraints[13] were applied. The constraints are necessary to ensure that the proton that is attached to the C atom of the model substrate is not pointing to the oxygen atom of the water molecule to form an unwanted H-bond. In a polypeptide, this would, of course, not be a concern. In the intermediate state optimized with the two constraints, one proton initially attached to the $O_{\delta 2}$ atom of the active site was transferred to the substrate so that the substrate forms two hydrogen bonds with the active site after optimization. In addition, significant rearrangement of the hydrogen bond involving one of the hydrogen atoms of the water molecule occurred. This hydrogen atom, which is originally H-bonded to the $O_{\delta 2'}$ atom, loses its original hydrogen bond to form a new H-bond across the active site to $O_{\delta 1}$. Overall, one proton is transferred (Figure 1, INT).

3. Second Transition State (TS_2). Following the intermediate state is the second transition state. This transition state is associated with the nucleophilic attack of the water molecule on the C atom of the substrate, and is crucial for the collapse of the substrate. This transition state was achieved by a number of optimizations (about 20) for each of which the reaction coordinate (RC), the distance between the oxygen atom (of the water molecule) and the carbon (of the substrate), was fixed while relaxing the remainder of the system. For a set of different RC distances, the transition state becomes the local energy maximum. The bisection rule was applied (from 1.4 to 2.2 Å) to this reaction coordinate during optimizations to select the desirable RC values efficiently. The actual transition state was finally obtained by the eigenvalue-following method (Figure 1, TS_2). At the RHF/6-31G* level, this reaction coordinate is approximately 1.50 Å at optimization and the energy barrier is approximately 10 kcal/mol above the INT minimum. This transition state structure is somewhat similar to the preceding intermediate state (INT).

4. Final State (FS). The collapse of the substrate occurs when the reaction coordinate (RC) distance C$-$O is shortened below its critical value of 1.50 Å with the final state FS connected to TS_2. We then began a full optimization with no constraints to initiate the hydrolysis, from the TS_2 geometry with RC slightly below 1.50 Å. A steep energy drop occurred during which the substrate collapsed, accompanied by a proton transfer which involves one of the protons originally attached to the water oxygen atom to the $O_{\delta 1}$ of the active site. This process is depicted in detail in Figure 1 (FS). The downhill energy drop is approximately 34 kcal/mol. Consequently, the overall reverse reaction is unfavorable. Up to this step, the fragments of the substrate remain attached to the active site. It is interesting that the formic acid fragment of the cleaved product is attached to both aspartic acid side chains by H-bonds, as suggested by Jaskolski *et al.*,[9] although in a somewhat different manner.

5. Cyclic States (CS). Here the HIV-PR returns to its starting state to complete the hydrolysis cycle. We calculated this "product release" cycle in two distinct steps to return the active site motif back to initiation. The key in the first step appears to be the removal of the amino-terminal product since it is weakly attached to the active site by a long hydrogen bond. The optimization for this step was started by deleting the amino terminus from the optimized structure of the previous step and optimizing with no constraints. The optimized structure is similar to the corresponding part in the previous structure. Removing the product fragment has an energy cost of about 5 kcal/mol, approximately the loss of a single hydrogen bond. This structure is described in detail in Figure 1 (CS_1).

The removal of the C-terminal substrate is not straightforward as it involves the breakage of two hydrogen bonds. Our strategy was to put a new water molecule back in the system to start the minimization. The water molecule was constructed from the (FS) structure by turning the nitrogen atom of NH_3 into oxygen and by removing the NH_3 hydrogen that is most distant from the active site. This new system was then optimized in two steps: First, full optimization was performed with no constraints. This minimization leads to the breakage of one of the two remaining hydrogen bonds between the product and the active site. Also, one of the aspartic model side chains rotated approximately 180° during the optimization, resulting in a non-co-planar active site configuration. An interesting detail of this structure is that the 180° rotation of the aspartate model makes the alternation of the protonation states of the active site possible. Secondly, co-planar constraints of the active site side chains were once again provided while carefully maintaining all of the possible hydrogen-bond interactions to begin our final geometry optimization. The optimized structure, in fact, maintains all the hydrogen-bond interaction details from the non-co-planar structure. The removal of the C-terminal product then occurs by breaking the only remaining hydrogen bond that

(13) We wished to avoid the formation of a spurious hydrogen bond: (substrate) C$-$H$\cdots$O (water). Two constraints were employed on the substrate angles (**Z**-matrix form):

Hc	C	BOND_Hc	N	ANGLE_Hc	Hn	DIHEDRAL_Hc
Oc	C	BOND_Oc	N	ANGLE_Hc	Hn	$-$ DIHEDRAL_Hc

where the labels of these atoms are given in Figure 1 (INT). The parameters defining the geometry of H_c and O_c were optimized jointly as shown.

(14) The energy profiles of different computational levels are somewhat similar. The basis set (6-31G*) improves the description of hydrogen bonding (over 4-31G), and reverses the high$-$low barrier of the transition states TS_1 and TS_2 (Table 1). The low TS_2 energy barrier (1.5 kcal/mol) for the MP2//6-31G* single-point calculations is not surprising since the accurate height of this barrier will depend on locating the true MP2 level transition state. The correlation effect on the two energy barriers was estimated by BLYP/6-31G* density-functional (Becke exchange, Lee-Yang-Parr correlation) calculations using the implementation of Gaussian92/DFT. The correlation does not change our original description of the catalytic mechanism around the transition states (TS_1 and TS_2) qualitatively$-$BLYP increases the TS_1 barrier (relative to INI + GS) from 15.9 kcal/mol (HF/6-31G*) to 18.2 kcal/mol, while BLYP decreases the TS_2 barrier of 9.5 kcal/mol (HF/6-31G*, relative to INT) to 6.8 kcal/mol.

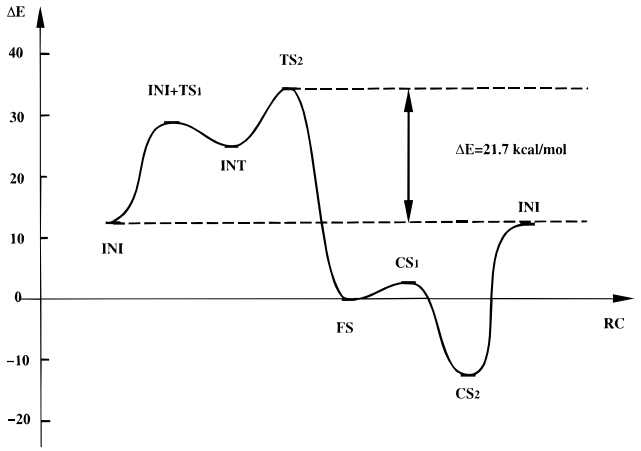

Figure 2. Energy profile (RHF/6-31G*) for the proposed reaction path. See text for definition of each reaction step.

Table 1. Energy Results for the *ab initio* Model[a]

reaction step substrate	ΔE (kcal/mol)[c]	reaction step substrate	ΔE (kcal/mol)[c]
TS_1 img freq[b]	505.3	TS_2	34.2
(INI + GS)	12.6	TS_2 img freq[b]	137.3
(INI + TS_1)	28.2	FS	0.0
INT	24.7	(C_1 + NH_3)	4.9
		CS_2	−9.2

[a] RHF/6-31G* energies with analytical forces are presented here. See text for the definitions of reaction steps. [b] Imaginary frequencies of transition states are in cm^{-1}. [c] Energy changes are relative to the FS reaction step with optimized energies at the RHF/6-31G* level. The relative energy difference of FS and CS_2 states is better evaluated through the GS state−CS_2 is 21.7 kcal/mol below the (GS+INI) state, therefore, 9.2 kcal/mol below FS.

connects it to the active site. The energy release was approximately 22 kcal/mol, indicating the cost of a strong H-bond with an O−H distance of 1.64 Å. This state is described in detail in Figure 1, CS_2.

A refinement of CS_2 was performed to calibrate the overall energy barrier by replacing the C-terminal product by acetic acid in the CS_2 step. With constraints similar to those to form the initial separated reactants, the cost to return to the initial state is approximately 18 kcal/mol.

The catalytic mechanism of HIV-PR based on our RHF/6-31G* calculations[14] is described in detail in Figures 1 and 2 and Table 1. Structural parameters are available upon request from the authors.

Results and Discussions

The catalytic mechanism of Jaskolski *et al.*[9] describes the possible steps in the HIV-PR reaction: an electrophilic attack (of the proton of the side chain $O_{\delta 2}$ on substrate N), a nucleophilic attack, and a distinct product release step. The electrophilic attack weakens the scissile peptide bond (bond stretches by approximately 0.08 Å) and facilitates a tighter binding between the substrate and the protease. The transition state that results is related to the nucleophilic attack of the water molecule and is responsible for the collapse of the substrate. Such a nucleophilic attack is shared by most proposals.[8]

In viewing the detailed *ab initio* geometries at each reaction step, the following can be concluded: (1) The PR catalysis mechanism may involve an asynchronized two-proton transfer. Upon completion of the reaction cycle, the protonation states of the two side chain aspartates are reversed.[4] The first proton transfer plays the role of charge redistribution between the first transition state and the intermediate state, and therefore is at least partly responsible for the rearrangement of the hydrogen bond network between these states, whereas the second proton transfer is partly responsible for the alternation of the protonation states of the two aspartates between the final state and the regenerated initial state. (2) The intermediate state (INT) is a vital part of the catalysis. Along the reaction path, this state bridges the two transition states in such a way that the entire hydrogen bond network does not alter significantly in proceeding from the intermediate state to the second transition state (TS_2). (3) Based on the fact that proline is the most commonly observed residue at the $P_{1'}$ scissile position in the substrates for aspartic proteases,[15] our catalytic proposal may provide a possible explanation: proline is the only residue whose main-chain nitrogen atom naturally adopts the tetrahedral conformation as in the TS_1 transition state. Proline at $P_{1'}$ does not need to adjust significantly to assume the TS_1 transition state as other residues must; therefore the forward energy barrier for proline at $P_{1'}$ is significantly reduced. On the other hand, one must keep in mind that the substrate formamide molecule in this study does introduce an extra hydrogen bond more than proline would, in both INT and TS_2 states.

In comparing the *ab initio* mechanism with Jaskolski *et al.*'s proposal, we were able to confirm the direction of the electrophilic attack, as suggested by Jaskolski *et al.*,[9] although we do not find a concerted electrophilic and nucleophilic attack mechanism. In fact, we find that these steps are separated by an intermediate state (Figure 1, INT). In addition, the collapsed acetyl-terminal (FS) was found to be hydrogen bonded to the inner oxygen atoms of the aspartic side chains.[9] We have proposed a subsequent product release step (CS_1 and CS_2) that involves an additional water molecule from the solvent. This step is an accord with the conclusion of a kinetic isotope

Table 2. Structural Parameters of the *ab Initio* Model[a]

reaction steps	planarity of D25/D25′,[b]	distance of C_γ−$C_{\gamma'}$, Å
INI	180	6.54
INT	125	5.69
TS_2	113	5.36
FS	121	6.10
CS_1	104	6.33
CS_2	180	6.63

Z-Matrix (Å and deg) of Transition State TS_2

1	H						
2	H	1	3.195677				
3	C	2	1.097720	1	22.757		
4	O	3	1.222190	2	117.329	1	−179.459
5	O	3	1.251618	2	114.132	4	180.296
6	O	5	5.184082	3	88.285	4	−26.386
7	C	6	1.233211	5	76.293	3	−141.869
8	H	7	1.102373	6	115.920	5	156.053
9	O	7	1.238217	6	128.864	8	179.783
10	O	9	2.629577	7	122.281	6	−2.086
11	H	10	0.990864	9	3.884	7	138.608
12	C	10	1.500868[c]	11	112.020	9	10.885
13	N	12	1.583181	10	99.830	11	63.313
14	N	13	1.023134	12	108.760	10	55.945
15	H	13	1.003992	12	106.523	10	172.378
16	H	13	1.027240	12	112.426	10	−66.797
17	O	12	1.230467	10	115.376	11	−175.980
18	H	12	1.092926	10	101.735	11	−42.636

[a] Lengths are in angstroms, angles in degrees. Geometries are from the optimized structures for the RHF/6-31G* basis. The structures of the formamide molecules are found in ref 12. Detailed parameters of each reaction step are available upon request from the authors. [b] Defined as the angles between the normal vectors of D25 and D25′ planes (180° = planar active-site motif0. [c] The reaction coordinate (RC).

(15) Meek, T. D. *J. Enzyme Inhib.* **1992**, *6*, 65−98.

experiment[4b] that a second water molecule is involved in the product release. Most importantly, our *ab initio* calculations agree with the long-standing hypothesis[8,9] that the nucleophilic attack of the lytic water to the scissile-bond carbon leads to a transition state that is responsible for the collapse of the substrate.

The $C_\gamma-C_\gamma$ distances in our calculations are 6.5 (INI), 5.7 (INT), 5.4 (TS_2), 6.1 (FS), 6.3 (CS_1), and 6.6 Å (CS_2), respectively, while the X-ray structures of the wild-type aspartic protease showed a range of 5.3 (HIV-1 PR) to 5.8 Å (chymosin). A protease−substrate complex usually has smaller $C_\gamma-C_\gamma$ distance (4.9 Å in ref 9, for example); we see the same trend in our calculated structures. The larger $C_\gamma-C_\gamma$ distances of several steps in our calculations are most likely due to the size of our model. In the INT and TS_2 structures, the aspartate side chains are somewhat rotated so as to bind the substrate (Table 2); the rotated forms then fit well into the binding cavity. In the CS_2 step, the formic acid fragment from the collapsed substrate is only hydrogen bound to the $O_{\delta 1}$ of D25; it costs very little energy to rotate it into an unoccupied space in the binding pocket.

We conclude that there are five distinct stages in the HIV-PR catalytic reaction pathway. Although largely consistent with existing experimental findings, this model must be improved to involve the residues that are in immediate contact with the active site aspartic acids. The details of enzymatic specificity will surely involve an expanded transition state for both the substrate and the catalyst. Understanding the catalytic mechanism hopefully will provide vital information for the design of drugs that inhibit the protease.

Note Added in Proof: Since the submission of our paper, an ab initio study has appeared [Silva, A.; Cochau, R.; Sham, H.; Erickson, J. *J. Mol. Biol.* **1996**, *255*, 321−346] that finds an activation energy of ∼50 kcal/mol for the hydrolysis of *N*-methylacetamide.

Acknowledgment. H.L. thanks the NIEHS intramural research office for a research fellowship provided through the NIEHS/NIH intramural program. We are indebted to the generous provisions of computing time from Cray Research, Inc., the Frederick computer center of NIH, and North Carolina Supercomputer Center. We thank Howard Smith for graphic representation and analysis.

Supporting Information Available: Tables of energy and structure data (8 pages). This material is contained in many libraries on microfiche, immediately follows this article in the microfilm version of the journal, can be ordered from the ACS, and can be downloaded from the Internet; see any current masthead page for ordering information and Internet access instructions.

JA9513188